

Decay of the low-energy nuclear ^{229m}Th isomer via atomic Rydberg states

E. V. Tkalya^{1,2,3,*}

¹*P.N. Lebedev Physical Institute of the Russian Academy of Sciences, 119991, 53 Leninskiy pr., Moscow, Russia*

²*National Research Nuclear University MEPhI, 115409, Kashirskoe shosse 31, Moscow, Russia*

³*Nuclear Safety Institute of RAS, Bol'shaya Tulkaya 52, Moscow 115191, Russia*

(Dated: April 30, 2020)

In the paper, a unique process of the decay of the $^{229m}\text{Th}(3/2^+, 8.28 \pm 0.17 \text{ eV})$ low energy nuclear isomer via the internal conversion (IC) channel on Rydberg states is considered for the first time. The Rydberg atom $^{229m}\text{Th}^+ + e_{Ry}^-$ is a unique object where IC is possible exclusively on the Rydberg electron e_{Ry}^- . It is shown that in the $^{229m}\text{Th}^{4+} + e_{Ry}^-$ system a) IC on the electron states with relatively small values of the principal quantum number n and the orbital moment l is practically completely suppressed, b) IC probability, W_{IC} , on the $\psi_{ns_{1/2}}(\mathbf{r})$ states is proportional to $|\psi_{ns_{1/2}}(0)|^2$ and can be related with the energy of the hyperfine interaction of the Rydberg electron with the nucleus, c) W_{IC} decreases rapidly with the increase of n in the range from 10 to 50, and in the range $n \gtrsim 150$ W_{IC} changes as Const/n^3 typical for hydrogen-like ions, d) at $n \approx 10\text{--}30$, W_{IC} as a function of l has a characteristic “knee” between $l = 3$ and $l = 4$, i.e. a three order of magnitude decrease of W_{IC} due to the qualitative change in the ratio between the centrifugal and shielding potentials.

PACS numbers: 23.20.Nx, 23.35.+g, 32.80.Ee

I. INTRODUCTION

The ^{229}Th ground-state doublet known since the mid-70s [1] is still a great challenge for traditional nuclear physics. Experimental studies of the past 30 years have shown that the energy E_{is} of the first excited state $^{229m}\text{Th}(3/2^+, E_{\text{is}})$ probably does not exceed 10 eV [2–8]. Such an unusually small for the nuclear scale excitation energy leads to the appearance of decay channels of ^{229m}Th uncharacteristic for the nuclear spectroscopy.

Among them, it is worth mentioning the internal conversion (IC) on the valence shells [9] and excited atomic states [9, 10], the nuclear radiation of the optical range in dielectrics with a large band gap [11, 12], electronic bridge [9, 13–19], α decay of ^{229m}Th [20], decay of ^{229m}Th in a metal via conduction electrons [21], dependence of ^{229m}Th decay rate on the boundary conditions [22], partial inversion of the doublet levels and the decay of the ground state at the muonic atom $(\mu_{1S_{1/2}}^{229}\text{Th})^*$ [23], and others.

At present, the ^{229m}Th IC decay in atomic Th was confirmed and the half-life of the excited state was estimated [5, 6], the magnetic dipole and electric quadrupole moments of the isomeric level were measured and the charge radius of ^{229m}Th was determined [24].

The importance of comprehensive studies of low-lying doublet levels in ^{229}Th is related to the possibility of developing the nuclear time standard [25–28], creating a γ -ray laser in the optical range [29, 30], measurements of the variation of strong interaction parameter [31, 32] and the fine structure constant [33], observations of the

cooperative spontaneous emission Dicke [29, 34] and the Mössbauer effect in the optical range [29].

In this work, another important channel of the decay of the ^{229m}Th isomer is investigated — the internal conversion on the Rydberg electrons e_{Ry}^- in the $^{229m}\text{Th}^{3+}$ ion (i.e. in the $^{229m}\text{Th}^{4+} + e_{Ry}^-$ system). Note that Rydberg atoms are well studied objects of modern physics (see, for example, the reviews [35–37] and references therein). Rydberg states in the Th ions were investigated, in particular, in the papers [38–40]. Therefore, the processes considered here in Th ions can be relatively easily studied with the modern experimental equipment. In addition, at IC process on the Rydberg states with large values of the principal quantum number, the energy of the emitted electron will practically coincide with the energy of the nuclear transition. This simplifies the measurement of the nuclear isomer energy and the interpretation of the experimental results.

II. FEATURES OF IC ON HIGHLY EXCITED STATES IN ^{229}Th

The ^{229m}Th isomer is the only object in which one can observe IC on the Rydberg states in a non-ionized atom. The reason is as follows. IC probability on the Rydberg states is vanishingly small compared to either the usual IC, or the probability of γ radiation at the decay of nuclear levels with excitation energy from a few to hundreds of kiloelectronvolts. Everything is different with ^{229m}Th .

When one of the $(6d_{3/2})^2(7s_{1/2})^2$ valence electrons of Th goes into an excited state, the absolute value of binding energy of the remaining electrons increases and at some point (when a valence electron goes into

*Electronic address: tkalya.e@lebedev.ru

a highly excited state) it becomes larger than the energy of the nuclear transition. For the currently accepted value $E_{is} \approx 8.28$ eV [8], the excitation of the valence $7s_{1/2}$ electron of the Th atom, say, to the $9s_{1/2}$ state is enough to completely stop IC process from all other levels including the valence $6d_{3/2}$ and $7s_{1/2}$ states because in the excited atom Th with the electron configuration $(6d_{3/2})^2(7s_{1/2})^1(9s_{1/2})^1$ the binding energy of the $6d_{3/2}$ electrons is approximately -10.3 eV, and the binding energy of the $7s_{1/2}$ electron is -9.6 eV. I.e. the binding energy of electrons at these states becomes greater than the energy of the isomeric nuclear transition. And IC decay from the $6d_{3/2}$ and $7s_{1/2}$ states in the excited atom Th with the electron configuration $(6d_{3/2})^2(7s_{1/2})^1(9s_{1/2})^1$ is forbidden by the energy conservation law. The same is true and for the excitation of the valence $6d_{3/2}$ electron, say, to the $9p_{1/2}$ state. In the excited atom Th with the electron configuration $(6d_{3/2})^1(7s_{1/2})^2(9p_{1/2})^1$ the binding energy of the $6d_{3/2}$ electron is approximately -11.6 eV, and the binding energy of the $7s_{1/2}$ electrons is -10.1 eV. Therefore, IC from these states is forbidden. And of course the above is true if we excite one of the electrons to the highly excited Rydberg state. The remaining electrons of the atomic shell are not involved in IC.

In Th ions the ionization energy of 11.9 eV is reached already in Th^+ . Therefore, the decay of the $^{229m}\text{Th}^+$ isomer via IC channel is possible only on excited electronic states whose binding energy E_b satisfies the condition $|E_b| < E_{is}$. The same will take place in the multiply charged Th ions.

The electronic bridge mentioned above can be an alternative process (or competitor) to IC process on the Rydberg states in ^{229}Th . However, it is expected that it depends critically on of the magnitude of the detuning between the energies of the nuclear and the associated atomic transition. Therefore, the electronic bridge will be the dominant decay channel only if favorable conditions are met in the atom or ion for resonant transfer of the excitation energy from the nucleus to the electron shell.

III. WAVE FUNCTIONS OF THE RYDBERG STATES IN SCREENED COULOMB POTENTIAL

Th ions can be trapped and then measured with a high accuracy in these ion traps [24, 41–45]. Therefore, I will consider IC on the Rydberg electron e_{Ry}^- in the $^{229m}\text{Th}^{3+}$ ion, which is the $^{229m}\text{Th}^{4+} + e_{Ry}^-$ system (that is, the $^{229m}\text{Th}^{4+}$ ion with an electron on a Rydberg state orbit). The Th^{4+} ion has the completely filled shell isoelectronic with that of the Rn atom, which is weakly polarized by the Rydberg electron [40, 46]. A corresponding small change of the electron density does not affect practically (after double integration) the potential whose stems from the undisturbed electron core of Th^{4+} , and consequently the Rydberg WF and the probability of IC

leave unchanged.

I consider here two cases, namely, the Rydberg states with large and small values of the orbital moment l . I will call “large” the values of l for which the Rydberg electron does not penetrate into the region of the electron core, i.e. to the region occupied by the shell electrons of the Th^{4+} ion [35].

In a hydrogen-like ion with a point nucleus of charge Z_{nucl} the potential energy of electron is [47]

$$V_{\text{H-like}}(x) = -\varepsilon_0 \frac{Z_{\text{nucl}}}{x} + V_l(x),$$

where $\varepsilon_0 = me^4$ is the atomic unit of energy (m is the electron mass, $-e$ is the electron charge, the system of units is $\hbar = c = 1$), $x = r/a_B$, a_B is the Bohr radius,

$$V_l(x) = \varepsilon_0 \frac{l(l+1)}{2x^2}$$

is electron energy at centrifugal potential. The bound state of an electron with the principal quantum number n and the orbital moment l has in this potential two regions forbidden for the classical motion [35]: the first region,

$$x > \frac{n^2}{Z} \left(1 + \sqrt{1 - \frac{l(l+1)}{n^2}} \right),$$

always exists in the Coulomb potential, and the second region,

$$0 < x < \frac{n^2}{Z} \left(1 - \sqrt{1 - \frac{l(l+1)}{n^2}} \right),$$

appears due to the centrifugal potential when $l \geq 1$.

In Th^{4+} the characteristic size of the electron core is approximately $2a_B$ [46]. Therefore, for each n there is a value l , when the damped wave functions almost do not penetrate the electron core. In this case, one can use for calculations the electron wave functions for the potential from the point nuclear charge [35].

Such functions are well known — these are the Dirac bispinors [48]. The large $g_i(x)$ and small $f_i(x)$ components of the Dirac bispinor of a bound (initial) electron state, normalized by the condition $\int_0^\infty [g_i^2(x) + f_i^2(x)]x^2 dx = 1$, in the Coulomb potential of the effective point charge Z_{ion} (in our case $Z_{\text{ion}} = 4$), have the form

$$\begin{aligned} \begin{pmatrix} g_i(x) \\ f_i(x) \end{pmatrix} &= -\frac{\sqrt{\Gamma(2\gamma_i + n_r + 1)}}{\Gamma(2\gamma_i + 1)\sqrt{n_r!}} \sqrt{\frac{1 \pm E_b/m}{4N(N - \kappa_i)}} \times \\ &(2Z_{\text{ion}}/N)^{3/2} e^{-Z_{\text{ion}}x/N} (2Z_{\text{ion}}x/N)^{\gamma_i - 1} \times \\ &[n_r F(-n_r + 1, 2\gamma_i + 1, 2Z_{\text{ion}}x/N) \mp \\ &(N - \kappa_i) F(-n_r, 2\gamma_i + 1, 2Z_{\text{ion}}x/N)], \quad (1) \end{aligned}$$

where $\kappa_i = l_i(l_i + 1) - j_i(j_i + 1) - 1/4$, l_i and j_i are the orbital and total electron momentum in the initial state,

$E_b = m/\sqrt{1 + [Z_{\text{ion}}e^2/(\gamma_i + n_r)]^2}$ is the energy of the bound electron, $n_r = n - |\kappa_i|$, $N = \sqrt{n^2 - 2n_r(|\kappa_i| - \gamma_i)}$, $\gamma_i = \sqrt{\kappa_i^2 - (Z_{\text{ion}}e^2)^2}$, $F(a, b, c)$ and $\Gamma(d)$ are the confluent hypergeometric and the gamma functions respectively [49].

The wave functions of the continuous spectrum normalized at $x \rightarrow \infty$ with the condition $g_f(x) = i^{l_f} \sin(pa_B x - \pi l_f/2)/x$ have the form [48]

$$\begin{aligned} \begin{pmatrix} g_f(x) \\ f_f(x) \end{pmatrix} &= \frac{e^{\pi(\xi + il_f)/2} |\Gamma(\gamma_f + i\xi)|}{x \Gamma(2\gamma_f + 1)} e^{2i\eta} \times \\ &\quad (2pa_B x)^\gamma \left(\frac{1}{\sqrt{(E_c - m)/(E_c + m)}} \right) \times \\ &\quad \begin{pmatrix} \text{Re} \\ \text{Im} \end{pmatrix} [(\gamma_f + i\xi) e^{i\eta} e^{-ipa_B x} \times \\ &\quad F(\gamma_f + 1 + i\xi, 2\gamma_f + 1, 2ipa_B x)], \quad (2) \end{aligned}$$

where γ_f and κ_f are defined through the orbital l_f and the total j_f electron moments of the final state similarly to the parameters γ_i and κ_i introduced earlier, $\exp(2i\eta) = (\gamma_f - i\xi)/(-\kappa_f - i\xi m/E_c)$, E_c and p are the energy and momentum of the conversion electron satisfying the condition $E_c^2 = m^2 + p^2$, $\xi = Z_{\text{ion}}e^2 E_c/p$.

Electronic states with lower values of l have significant amplitudes inside the electron core. Therefore, such WFs of the initial bound state with the electron energy $E < m$ as well as the final state of the continuous spectrum with $E > m$ were calculated from the Dirac equations

$$\begin{aligned} \frac{dg(x)}{dx} + \frac{1 + \kappa}{x} g(x) - \frac{1}{e^2} \left(\frac{E}{m} + 1 - \frac{V(x)}{m} \right) f(x) &= 0, \\ \frac{df(x)}{dx} + \frac{1 - \kappa}{x} f(x) + \frac{1}{e^2} \left(\frac{E}{m} - 1 - \frac{V(x)}{m} \right) g(x) &= 0. \end{aligned} \quad (3)$$

Here

$$V(x) = V_{\text{nucl}}(x) + V_{\text{shell}}(x),$$

where $V_{\text{nucl}}(x)$ is the potential energy of electron in potential of the unscreened nucleus, and $V_{\text{shell}}(x)$ is the potential energy of the electron in the potential of the shell electrons.

As $V(x)$, one can use approximate expressions for the many-electron atoms potential from the work [50] or solve the Poisson equation. In the present work, the second approach is chosen.

The electron potential energy inside and outside nucleus has been calculated by taking the ^{229}Th nucleus in the spherical approximation. That is, the positive charge of the nucleus has been uniformly distributed within a sphere of the radius $x_{R_0} = R_0/a_B$ ($R_0 = 1.2A^{1/3}$ fm is the radius of the nucleus with the atomic number A). One finds that

$$V_{\text{nucl}}(x) = \begin{cases} -\varepsilon_0 \frac{Z_{\text{nucl}}}{2x_{R_0}} \left[3 - \left(\frac{x}{x_{R_0}} \right)^2 \right] & \text{for } 0 \leq x \leq x_{R_0}, \\ -\varepsilon_0 \frac{Z_{\text{nucl}}}{x} & \text{for } x \geq x_{R_0}. \end{cases}$$

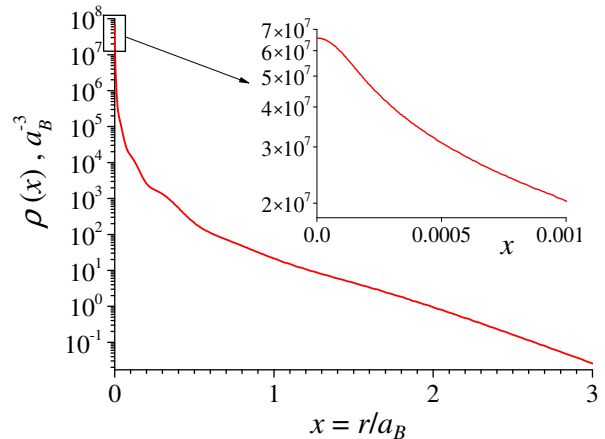


Figure 1: Electron density of the Th^{4+} ion.

The electron shell potential $V_{\text{shell}}(x)$ has been found by solving the Poisson equation with the given electron density $\rho_e(x)$, Fig. 1. The electron density shown in Fig. 1 has been obtained for Th^{4+} within the DFT theory (with three different codes [51–54]) through the self-consistent procedure taking into account the exchange and correlation effects. The electron density for Th^{4+} satisfy the condition $\int_0^\infty \rho_e(x) x^2 dx = Z_{\text{nucl}} - Z_{\text{ion}} = 86$.

Note that the implemented approach automatically takes into account the so-called quantum defect (for more details, see in [35, 37]). Here, from the very beginning I am seeking the WFs and energies of the Rydberg states with the quantum number n as solutions of the Dirac equation (3) in the potential $V(x)$, which takes into account the electron shell of the ionic core. So no renormalization of n required.

IV. INTERNAL CONVERSION ON THE $ns_{1/2}$ RYDBERG STATES

The main contribution to IC on the $ns_{1/2}$ states in the ^{229m}Th decay comes from the $M1$ multipole [9]. This is valid for IC on all electronic $ns_{1/2}$ states including excited states [9, 10, 55] for the entire known range of the reduced probabilities of the nuclear transition $0.006 \leq B_{\text{W.u.}}(M1, 3/2^+ \rightarrow 5/2^+) \leq 0.04$, $6 \leq B_{\text{W.u.}}(E2, 3/2^+ \rightarrow 5/2^+) \leq 29$ [10, 56]. The purpose of this Section is to estimate the probability of IC on the $ns_{1/2}$ Rydberg states and give an approximate estimate of the magnitude of the corresponding internal conversion coefficients (ICC). Therefore, here I focus mainly on the discussion of the $M1$ internal conversion.

ICC for the $E(M)L$ transition is given by the formula

$$\begin{aligned} \alpha_{E(M)L} &= \frac{\omega_N}{p} \frac{E_c + m}{m} \frac{L}{L + 1} \sum_{l_f, j_f} |\mathcal{F}^{E(M)L}(l_i, j_i, l_f, j_f)| \\ &\quad \times |\mathcal{M}_{if}^{E(M)L}|^2, \quad (4) \end{aligned}$$

where functions $\mathcal{F}^{E(M)L}$ are defined by the relations

$$\begin{aligned} \mathcal{F}^{EL}(l_i, j_i, l_f, j_f) &= (-1)^{2j_f+1} (2j_f+1)(2l_i+1) \times \\ &\quad \left(C_{L0l_i0}^{l_f0} \right)^2 \begin{pmatrix} L & l_i & l_f \\ 1/2 & j_f & j_i \end{pmatrix}^2, \quad (5) \\ \mathcal{F}^{ML}(l_i, j_i, l_f, j_f) &= \mathcal{F}^{EL}(l'_i, j_i, l_f, j_f). \end{aligned}$$

where $C_{10l_i0}^{l_f0}$ is the Clebsch-Gordan coefficient followed in Eq. (5) by the $6j$ symbol, $l'_i = 2j_i - l_i$. The electron matrix elements in Eq. (4) are

$$\begin{aligned} \mathcal{M}_{if}^{EL} &= \int_0^\infty dx x^2 h_L^{(1)}(\omega_N a_B x) [g_i(x) g_f(x) + \\ &\quad f_i(x) f_f(x)], \quad (6) \\ \mathcal{M}_{if}^{ML} &= \frac{\kappa'_i - \kappa_f}{L+1} \int_0^\infty dx x^2 h_L^{(1)}(\omega_N a_B x) \times \\ &\quad [g_i(x) f_f(x) + f_i(x) g_f(x)]. \end{aligned}$$

Here $h_L^{(1)}(\omega_N a_B x)$ is the Hankel function of the first kind [49], $\kappa'_i = l'_i(l'_i+1) - j_i(j_i+1) - 1/4$.

The matrix elements (6) were calculated by numerical integration using analytical wave functions, Eqs. (1) and (2), and numerical solutions to Eq. (3). Although there are cases of successful analytical calculation of similar electronic matrix elements for some nonrelativistic WFs of the Rydberg states [57, 58], in our case it is easier to use a unified approach for the both types of WFs present in the problem.

Usually the main contribution to IC comes from the static multipole zone near the nucleus, where the Hankel function in Eq. (6) has a pole $h_L^{(1)}(z) \sim 1/z^{L+1}$. The $M1$ internal conversion is most likely on the $ns_{1/2}$ states with the maximum amplitude at the nucleus. In addition, the final $S_{1/2}$ state of the continuous spectrum, which also has a largest amplitude in the nucleus region, is one of the states allowed by the selection rules for the $M1$ internal conversion on the $ns_{1/2}$ states. That is the internal conversion on the $ns_{1/2}$ states give an upper estimate for IC probability on the Rydberg levels and, accordingly, a lower bound for the nuclear isomer lifetime.

Calculated IC coefficient α_{M1} as a function of the main quantum number n on the Rydberg states $ns_{1/2}$ in the $\text{Th}^{4+} + e_{Ry}^-$ system is presented in Fig. 2. Up to $n = 500$, the Dirac equation (3) was solved numerically. Using the obtained data one can extrapolate the behavior of $\alpha_{M1}(ns_{1/2})$ to larger values of n . For $n \gtrsim 150$ one finds that $\alpha_{M1}(ns_{1/2}) \sim \text{Const}/n^3$. This conclusion is supported by the fact that in the non relativistic case for any fixed l_i the square of the modulus of the matrix element $\langle f|r^{-2}|i\rangle$ for the transition from the bound state to the continuum is proportional to n^{-3} [35]. In addition, as shown in the inset in Fig. 2, $\alpha_{M1}(ns_{1/2})$ is proportional to the square of $g_{ns_{1/2}}(0)$ (which is the amplitude of WF at $x = 0$), that is, within the accuracy of our calculation $\alpha_{M1}(ns_{1/2})/g_{ns_{1/2}}^2(0) = c_1$, where $c_1 =$

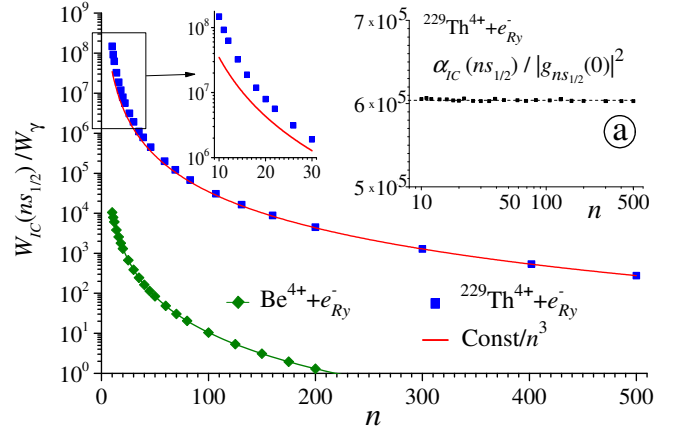


Figure 2: Internal conversion coefficients for the $ns_{1/2}$ states. Blue squares are the results for $^{229m}\text{Th}^{4+} + e_{Ry}^-$ (Dirac calculations), the red connecting line is given by $\alpha_{IC}(300)/(n/300)^3$. The right panel inset (a) demonstrates that $\alpha_{M1}(ns_{1/2}) \propto g_{ns_{1/2}}^2(0)$. Green rhombuses connected by the green line at the left lower panel are the hydrogen-like model results for the $M1$ transition with 8.28 eV in $\text{Be}^{4+} + e_{Ry}^-$.

6.03×10^5 . Taking into account that for the hydrogen-like ions $g_{ns_{1/2}}(0) \propto (Z_{\text{ion}}/n)^{3/2}$, one obtains again the same dependence on n . In particular, for the case of the hydrogen-like Be atom (i.e. the $\text{Be}^{4+} + e_{Ry}^-$ system with $Z_{\text{Be}} = 4$) one obtains for $n \geq 10$ for the IC coefficient the following relation $\alpha_{M1}(ns_{1/2}) = 1.03 \times 10^7/n^3$ (see in Fig. 2). This relation was calculated with the analytical WFs (1)–(2) for a model nuclear $M1$ transition with the energy of 8.28 eV.

On the other hand, the IC probabilities for the $ns_{1/2}$ wave functions and the other states penetrate the electron core deviate from that for the hydrogen-like ions. For example, IC coefficients for $\text{Th}^{4+} + e_{Ry}^-$ and $\text{Be}^{4+} + e_{Ry}^-$ shown in Fig. 2 are very different. Even for very large n , such WFs feel a charge distribution inside the electron core, which leads to different values for electron matrix elements. In the region of $n = 10 - 50$ the influence of the Th^{4+} electron core near the nucleus (where the $ns_{1/2}$ states feel a huge charge of ^{229}Th) is especially strong. With the increase of n , the average radius of the $ns_{1/2}$ state increases as n^2/Z_{eff} (Rydberg electron is moved in effective potential created by the effective charge Z_{eff}), and the screening of the nucleus is strengthening. It leads to a rapid decrease of Z_{eff} and effective potential. As a result, both $|g_{ns_{1/2}}(0)|^2$ and the IC probability more fast decrease with n in $\text{Th}^{4+} + e_{Ry}^-$ in comparison with $\text{Be}^{4+} + e_{Ry}^-$ (see the deviation the IC probability from the n^{-3} law in $\text{Th}^{4+} + e_{Ry}^-$ in the left top panel inset in Fig. 2).

The calculation of IC probability for the $E2$ multipole gives the same dependence of ICC as for the $M1$ case: $\alpha_{E2}(ns_{1/2}) \sim |g_{ns_{1/2}}(0)|^2 \propto n^{-3}$. Thus, the well known relationship between the probabilities

$W_{IC}^{M1}(ns_{1/2}) \gg W_{IC}^{E2}(ns_{1/2})$ for IC on the $ns_{1/2}$ states in the region of small n [9] is preserved for large values of n . Using the relations $\alpha_{M1}(ns_{1/2}) \sim \text{Const}/n^3$ and $W_{IC}^{M1}(ns_{1/2}) \gg W_{IC}^{E2}(ns_{1/2})$, one can find the value n , at which the probability of the internal conversion on the Rydberg state $ns_{1/2}$ becomes equal to the probability of the γ radiation upon the decay of the ^{229m}Th isomer. One obtains $n \simeq 3300$.

I note an interesting feature of the internal conversion on the $ns_{1/2}$ states. The Rydberg electron in the $ns_{1/2}$ state in the $^{229m}\text{Th}^{4+} + e_{Ry}^-$ or $^{229}\text{Th}^{4+} + e_{Ry}^-$ systems produces a magnetic field at the Th nucleus. The interaction of the ^{229}Th with this magnetic field in the ground state (which magnetic moment is $\mu_{gr} = 0.36$) or isomeric state ($\mu_{is} = -0.37$ [24]) leads to a splitting of nuclear levels. The energy of the sublevels with the quantum number F ($\mathbf{F} = \mathbf{I} + \mathbf{s}$, I stands for the nuclear spin, s is the electron spin) is determined by the formula for the Fermi contact interaction (see in [59])

$$E_F = E_{\text{int}} \frac{F(F+1) - I(I+1) - s(s+1)}{2Is},$$

with the interaction energy

$$E_{\text{int}} = \frac{8\pi}{3} \mu_{gr(is)} \mu_N \mu_B g_i^2(0),$$

where $\mu_B = e/2m$ is the Bohr magneton, $\mu_N = e/2M_p$ is the nuclear magneton, M_p is the proton mass.

Taking into account the relation $\alpha_{M1} = c_1 g_i^2(0)$ valid for $ns_{1/2}$, and expressing $g_i^2(0)$ by two different ways, one can obtain a relation between the hyperfine splitting energy E_F and the internal conversion coefficient α_{M1} , both of which are measured experimentally. This can be very helpful for additional verification of experimental results.

V. INTERNAL CONVERSION ON THE RYDBERG STATES WITH $l \geq 1$

The internal conversion on the shells with $l \geq 1$ differs from IC on the $ns_{1/2}$ shells. Along with the $M1$ multipole, the $E2$ multipole can make a significant contribution to the IC probability in ^{229m}Th on some shells with $l \geq 1$ as it was noted in [55].

The contributions of the multipoles depend on the values of the reduced probabilities of the nuclear transitions $B_{W.u.}(M1; 3/2^+ \rightarrow 5/2^+)$ and $B_{W.u.}(E2; 3/2^+ \rightarrow 5/2^+)$. To date, these values have not been measured. That is why one usually uses $B_{W.u.}(M1; 3/2^+ \rightarrow 5/2^+)$ and $B_{W.u.}(E2; 3/2^+ \rightarrow 5/2^+)$ obtained with Alaga rules from the available experimental data [60–63] for the $M1$ and $E2$ transitions between the rotation bands $3/2^+$ [631] and $5/2^+$ [633] (see in [56, 64]) either theoretical calculations [63, 65].

In the first case, the average values of the reduced nuclear transition probabilities are $B_{W.u.}(M1; 3/2^+ \rightarrow$

$5/2^+) = 3.1 \times 10^{-2}$ and $B_{W.u.}(E2; 3/2^+ \rightarrow 5/2^+) = 11.7$ [56], and the $E2$ component makes the main contribution to the IC process only on the $np_{3/2}$ shells: $W_{IC}(np_{3/2})/W_{IC}(ns_{1/2}) \approx 2.6$. For the $nd_{5/2}$ shells, the similar value is already less than 0.3, for the $nd_{3/2}$ shells it is less than 0.2, and for the rest shells, it is less than 0.1.

The calculation of the nuclear matrix elements of the low energy isomeric transition in ^{229}Th in the framework of the quasiparticle-plus-phonon model was done in [63], where the values $B_{W.u.}(M1; 3/2^+ \rightarrow 5/2^+) = 1.4 \times 10^{-2}$ and $B_{W.u.}(E2; 3/2^+ \rightarrow 5/2^+) \approx 67$ were predicted. Later, a more detailed and modern model, taking into account practically all known aspects of the nuclear forces, was used in [65]. This calculation gave $B_{W.u.}(M1; 3/2^+ \rightarrow 5/2^+) = 0.76 \times 10^{-2}$ and $B_{W.u.}(E2; 3/2^+ \rightarrow 5/2^+) \approx 27$. With these nuclear matrix elements, the contribution of the $E2$ multipole is an order of magnitude greater than the contribution of the $M1$ multipole for IC on the $np_{3/2}$ shells and is comparable with the $M1$ multipole for IC on the $nd_{5/2}$ and $nd_{3/2}$ shells. Therefore, here I will take into account the contribution to the IC of both $M1$ and $E2$ multipoles in Eqs. (4)–(6).

One finds that in the $^{229m}\text{Th}^{4+} + e_{Ry}^-$ system the IC probability decreases rapidly with increasing orbital angular momentum of the initial state l_i . Typical dependency is shown in Fig. 3 for $n = 21$. The wave functions of the initial and final states for $0 \leq l_i \leq 6$ were calculated by solving the Dirac equation (3). Also, analytical WFs, Eqs. (1)–(2), were used to calculate internal conversion coefficients for $0 \leq l_i \leq 8$ in the hydrogen-like model for Be. One has found that the results of both calculations lie very close for $l_i = 4$ while for $l_i = 5$ –6 the discrepancy is only about 1%. Notice that for $l_i = 8$ –9 the internal conversion process is practically suppressed.

Earlier in the introduction I have already discussed the mechanisms leading to the characteristic “knee” in Fig. 3 for $l_i = 3$ –4. The centrifugal potential growing as l_i^2 , at $l_i = 4$ exceeds the total potential of the nucleus and the electron shell when $0 \leq x \leq 2.5$ (Fig. 4). Therefore, in this region in the classical picture the motion with $l_i = 4$ is forbidden, while in the quantum case the wave functions become very small. This region however is responsible for a significant contribution to the IC matrix element, Eq. (6). (Since for the considered values of n and l_i the energy of Rydberg states is very close to zero, the boundary points of classical motion practically coincide with the intersection points of the centrifugal potential and total potential of the nucleus and the electron shell.) For $l_i \leq 3$ the situation is different. The total potential exceeds in magnitude the centrifugal potential already at $x \gtrsim 0.1$ (see Fig. 4). This leads to the formation of a potential well much closer to the nucleus than for the $l_i = 4$ case, and to significantly larger amplitudes of the electronic wave functions in the region responsible for a large contribution to the integral (6). As a result, the both the electron matrix element of the transition and

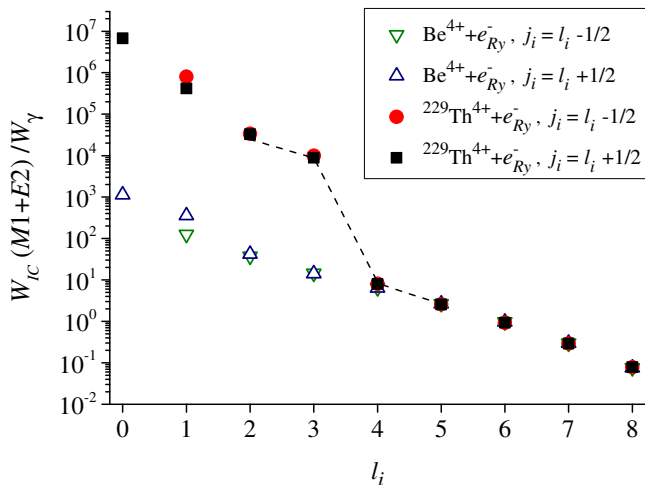


Figure 3: Internal conversion coefficient as a function of the orbital quantum number of the initial state l_i for $n = 21$ in the $^{229m}\text{Th}^{4+} + e^-_{Ry}$ system. The dashed line denotes the “knee” — a three order of magnitude drop of the internal conversion process between $l_i = 3$ and $l_i = 4$. (The reduced probabilities of the nuclear $M1$ and $E2$ transitions from work [56] were used for the calculations at $l_i = 1$ and 2.)

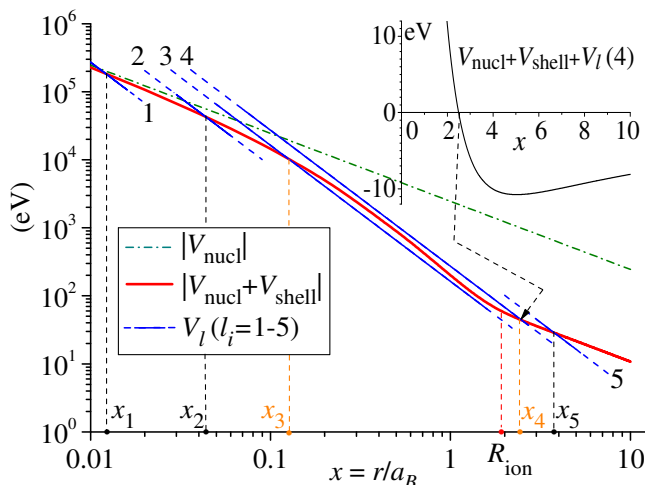


Figure 4: Relations between different types of potential energy. $V_{\text{nucl}}(x) = -\varepsilon_0 Z_{\text{Th}}/x$ is the potential energy of the Coulomb interaction of the ^{229}Th nucleus and the electron, $V_{\text{nucl}}(x) + V_{\text{shell}}$ is the energy of the Rydberg electron in the full potential (sum of the nucleus and the electron shell term from Eq. (3)), $V_l(x)$ is the Rydberg electron energy in the centrifugal potential for various orbital momentum l_i . R_{ion} is the size of the region occupied by the Th^{4+} ion. x_{l_i} ($l_i = 1-5$) are the points at which $|V_{\text{nucl}} + V_{\text{shell}}| = V_l$ (see example for $l_i = 4$ in the right panel inset).

IC probability become substantially larger.

The range of n and l_i values where IC probability in the $^{229m}\text{Th}^{4+} + e^-_{Ry}$ system exceeds the probability of γ radiation is shown in Fig. 5. We see that one can control the decay of the ^{229m}Th isomer by well known experimental methods at easy achievable values of $n =$

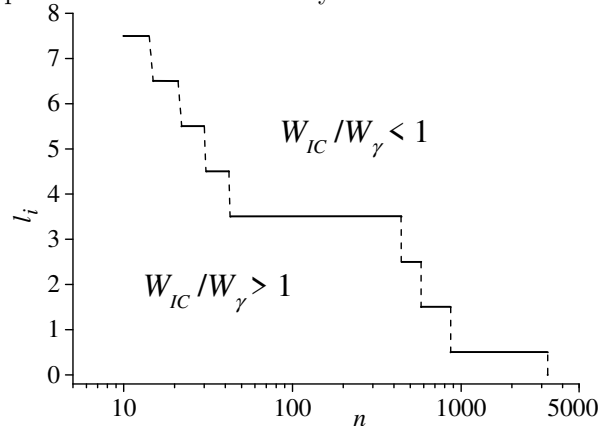


Figure 5: Relative intensities of the internal conversion and the γ radiation versus the n and l_i quantum numbers. Bottom left: the dominant channel is the internal conversion. Top right: the dominant channel is the γ radiation. Solid/dashed line: boundary values of n and l_i .

30–40 and $l_i = 4-6$.

Note in conclusion that for $l_i \geq 1$ the calculated IC probabilities also follow the n^{-3} law. This property of the electron matrix elements (see details in [35]) is helpful to control the accuracy of numerical calculation of WFs and matrix elements.

VI. CONCLUSION

Summing up, I have shown the possibility of observing experimentally a unique process — the decay of the low energy isomeric nuclear level in ^{229}Th via the channel of the internal conversion on the Rydberg states with a substantial (many orders of magnitude) increase of the lifetime of the ^{229m}Th isomer.

The author thanks Prof. N. N. Kolachevsky and Prof. V. S. Lebedev for helpful discussions. This research was supported by a grant of the Russian Science Foundation (Project No 19-72-30014).

- [1] L. A. Kroger and C. W. Reich, Nucl. Phys. A **259**, 29 (1976).
 [2] C. W. Reich and R. G. Helmer, Phys. Rev. Lett. **64**, 271 (1990).

- [3] R. G. Helmer and C. W. Reich, Phys. Rev. C **49**, 1845 (1994).
 [4] B. R. Beck, J. A. Becker, P. Beiersdorfer, G. V. Brown, K. J. Moody, J. B. Wilhelmy, F. S. Porter, C. A. Kil-

- bourne, and R. L. Kelley, Phys. Rev. Lett. **98**, 142501 (2007).
- [5] L. von der Wense, B. Seiferle, M. Laatiaoui, J. B. Neumayr, H. J. Maier, H. F. Wirth, C. Mokry, J. Runke, K. Eberhardt, C. E. Dullmann, et al., Nature **533**, 47 (2016).
- [6] B. Seiferle, L. von der Wense, and P. G. Thirolf, Phys. Rev. Lett. **118**, 042501 (2017).
- [7] T. Masuda, A. Yoshimi, A. Fujieda, H. Fujimoto, H. Haba, H. Hara, T. Hiraki, H. Kaino, Y. Kasamatsu, S. Kitao, et al., Nature **573**, 238 (2019).
- [8] B. Seiferle, L. von der Wense, P. V. Bilous, I. Amersdorfer, C. Lemell, F. Libisch, S. Stellmer, T. Schumm, C. E. Dullmann, A. Palffy, et al., Nature **573**, 243 (2019).
- [9] V. F. Strizhov and E. V. Tkalya, Sov. Phys. JETP **72**, 387 (1991).
- [10] P. V. Bilous, G. A. Kazakov, I. D. Moore, T. Schumm, and A. Palffy, Phys. Rev. A **95**, 032503 (2017).
- [11] E. V. Tkalya, JETP Lett. **71**, 311 (2000).
- [12] E. V. Tkalya, A. N. Zherikhin, and V. I. Zhudov, Phys. Rev. C **61**, 064308 (2000).
- [13] E. V. Tkalya, JETP Lett. **55**, 211 (1992).
- [14] P. Kalman and T. Keszthelyi, Phys. Rev. C **49**, 324 (1994).
- [15] S. G. Porsev, V. V. Flambaum, E. Peik, and C. Tamm, Phys. Rev. Lett. **105**, 182501 (2010).
- [16] S. G. Porsev and V. V. Flambaum, Phys. Rev. A **81**, 042516 (2010).
- [17] F. F. Karpeshin and M. B. Trzhaskovskaya, Phys. Rev. C **95**, 034310 (2017).
- [18] R. A. Muller, A. V. Volotka, and A. Surzhykov, Phys. Rev. A **99**, 042517 (2019).
- [19] P. V. Borisyuk, N. N. Kolachevsky, A. V. Taichenachev, E. V. Tkalya, I. Y. Tolstikhina, and V. I. Yudin, Phys. Rev. C **100**, 044306 (2019).
- [20] A. M. Dykhne, N. V. Eremin, and E. V. Tkalya, JETP Lett. **64**, 345 (1996).
- [21] E. V. Tkalya, JETP Lett. **70**, 371 (1999).
- [22] E. V. Tkalya, Phys. Rev. Lett. **120**, 122501 (2018).
- [23] E. V. Tkalya, Phys. Rev. A **94**, 012510 (2016).
- [24] J. Thielking, M. V. Okhapkin, P. Glowacki, D. M. Meier, L. von der Wense, B. Seiferle, C. E. Dullmann, P. G. Thirolf, and E. Peik, Nature **556**, 321 (2018).
- [25] E. Peik and C. Tamm, Europhys. Lett. **61**, 181 (2000).
- [26] W. G. Rellergert, D. DeMille, R. R. Greco, M. P. Hehlen, J. R. Torgerson, and E. R. Hudson, Phys. Rev. Lett. **104**, 200802 (2010).
- [27] C. J. Campbell, A. G. Radnaev, A. Kuzmich, V. A. Dzuba, V. V. Flambaum, and A. Derevianko, Phys. Rev. Lett. **108**, 120802 (2012).
- [28] E. Peik and M. Okhapkin, C. R. Phys. **16**, 516 (2015).
- [29] E. V. Tkalya, Phys. Rev. Lett. **106**, 162501 (2011).
- [30] E. V. Tkalya and L. P. Yatsenko, Laser Phys. Lett. **10**, 105808 (2013).
- [31] V. V. Flambaum, Phys. Rev. Lett. **97**, 092502 (2006).
- [32] E. Litvinova, H. Feldmeier, J. Dobaczewski, and V. Flambaum, Phys. Rev. C **79**, 064303 (2009).
- [33] J. C. Berengut, V. A. Dzuba, V. V. Flambaum, and S. G. Porsev, Phys. Rev. Lett. **102**, 210801 (2009).
- [34] R. H. Dicke, Phys. Rev. **93**, 99 (1954).
- [35] T. F. Gallagher, *Rydberg Atoms* (Cambridge University Press, New York, 2005).
- [36] N. Sibalic and C. S. Adams, *Rydberg Physics* (IOP Publishing, Bristol, UK, 2018).
- [37] V. S. Lebedev and I. L. Beigman, *Physics of Highly Excited Atoms and Ions* (Springer-Verlag, Berlin Heidelberg, 1998).
- [38] M. E. Hanni, J. A. Keele, S. R. Lundeen, and C. W. Fehrenbach, Phys. Rev. A **82**, 022512 (2010).
- [39] J. A. Keele, M. E. Hanni, S. L. Woods, S. R. Lundeen, and C. W. Fehrenbach, Phys. Rev. A **83**, 062501 (2011).
- [40] J. A. Keele, C. S. Smith, S. R. Lundeen, and C. W. Fehrenbach, Phys. Rev. A **85**, 064502 (2012).
- [41] C. J. Campbell, A. V. Steele, L. R. Churchill, M. V. DePalatis, D. E. Naylor, D. N. Matsukevich, A. Kuzmich, and M. S. Chapman, Phys. Rev. Lett. **102**, 233004 (2009).
- [42] C. J. Campbell, A. G. Radnaev, and A. Kuzmich, Phys. Rev. Lett. **106**, 223001 (2011).
- [43] O. A. Herrera-Sancho, N. Nemitz, M. V. Okhapkin, and E. Peik, Phys. Rev. A **88**, 012512 (2013).
- [44] M. V. Okhapkin, D. M. Meier, E. Peik, M. S. Safronova, M. G. Kozlov, and S. G. Porsev, Phys. Rev. A **92**, 020503(R) (2015).
- [45] K. Groot-Berning, F. Stopp, G. Jacob, D. Budker, R. Haas, D. Renisch, J. Runke, P. Thorle-Pospiech, C. E. Dullmann, and F. Schmidt-Kaler, Phys. Rev. A **99**, 023420 (2019).
- [46] E. Biemont, V. Fivet, and P. Quinet, J. Phys. B: At. Mol. Opt. Phys. **37**, 4193 (2004).
- [47] L. D. Landau and E. M. Lifshitz, *Quantum Mechanics. Non-relativistic Theory*. (Pergamon Press, New York, 1965).
- [48] A. I. Akhiezer and V. B. Berestetskii, *Quantum electrodynamics* (J. Wiley and Sons, New York, 1965).
- [49] M. Abramowitz and I. A. Stegun, *Handbook of Mathematical Functions* (National Bureau of Standards, Washington, D.C., 1964).
- [50] V. V. Flambaum and J. S. M. Ginges, Phys. Rev. A **72**, 052115 (2005).
- [51] A. A. Soldatov and D. P. Grechukhin, Kurchatov Institute of Atomic Energy Report-3174, Moscow, 1979.
- [52] I. M. Band and V. I. Fomichev, At. Data Nucl. Data Tabl. **23**, 295 (1979).
- [53] A. V. Nikolaev, The FLAPW-Moscow code, Registration No. 2015616990 (Russia) from 26/06/2015.
- [54] A. V. Nikolaev, D. Lamoën, and B. Partoens, J. Chem. Phys. **145**, 014101 (2016).
- [55] P. V. Bilous, N. Minkov, and A. Palffy, Phys. Rev. C **97**, 044320 (2018).
- [56] E. V. Tkalya, C. Schneider, J. Jeet, and E. R. Hudson, Phys. Rev. C **92**, 054324 (2015).
- [57] V. D. Ovsiannikov, A. Derevianko, and K. Gibble, Phys. Rev. Lett. **107**, 093003 (2011).
- [58] V. D. Ovsiannikov, I. L. Glukhov, and E. A. Nekipelov, Optics and Spectroscopy **111**, 25 (2011).
- [59] A. Abragam, *The Principles of Nuclear Magnetism* (Clarendon Press, Oxford, England, 1961).
- [60] C. E. Bemis, Jr., F. K. McGowan, J. L. C. Ford, Jr., W. T. Milner, R. L. Robinson, P. H. Stelson, G. A. Leander, and C. W. Reich, Phys. Scr. **38**, 657 (1988).
- [61] K. Gulda, W. Kurcewicz, A. J. Aas, M. J. G. Borge, D. G. Burkard, B. Fogelberg, I. S. Grant, E. Hagebo, N. Kaffrell, J. Kvasil, et al., Nucl. Phys. A **703**, 45 (2002).
- [62] V. Barci, G. Ardisson, G. Barci-Funel, B. Weiss, O. El Samad, and R. K. Sheline, Phys. Rev. C **68**, 034329 (2003).
- [63] E. Ruchowska, W. A. Plociennik, J. Zylicz, H. Mach,

- J. Kvasil, A. Algora, N. Amzal, T. Back, M. G. Borge, R. Boutami, et al., Phys. Rev. C **73**, 044326 (2006).
- [64] A. M. Dykhne and E. V. Tkalya, JETP Lett. **67**, 549 (1998).
- [65] N. Minkov and A. Palfy, Phys. Rev. Lett. **118**, 212501 (2017).